

See discussions, stats, and author profiles for this publication at: <https://www.researchgate.net/publication/258057604>

Prototropic and Photophysical Properties of Ellipticine inside the Nano-Cavities of Molecular Containers.

ARTICLE in THE JOURNAL OF PHYSICAL CHEMISTRY B · OCTOBER 2013

Impact Factor: 3.3 · DOI: 10.1021/jp408280p · Source: PubMed

CITATIONS

7

READS

57

4 AUTHORS, INCLUDING:



Krishna Gavvala

Indian Institute of Science Education and Res...

25 PUBLICATIONS 75 CITATIONS

[SEE PROFILE](#)



Raj kumar Koninti

Indian Institute of Science Education and Res...

15 PUBLICATIONS 44 CITATIONS

[SEE PROFILE](#)



Partha Hazra

Indian Institute of Science Education and Res...

52 PUBLICATIONS 997 CITATIONS

[SEE PROFILE](#)

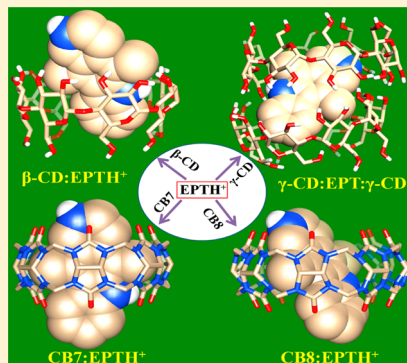
Prototypical and Photophysical Properties of Ellipticine inside the Nanocavities of Molecular Containers

Krishna Gavvala, Abhigyan Sengupta, Raj Kumar Koninti, and Partha Hazra*

Department of Chemistry, Mendeleev Block, Indian Institute of Science Education and Research (IISER), Pune 411008, Maharashtra, India

Supporting Information

ABSTRACT: Host–guest interactions between an anticancer drug, ellipticine (EPT), and molecular containers (cucurbiturils (CB_n) and cyclodextrins (CD)) are investigated with the help of steady state and time-resolved fluorescence measurements. Our experimental results confirm the formation of 1:1 inclusion complexes with CB_7 and CB_8 . The protonated form of EPT predominantly prevails in the inclusion complexes due to the stabilization achieved through ion–dipole interaction between host and positively charged drug. Drug does not form an inclusion complex with CB_6 , which is smaller in cavity size compared to either CB_7 or CB_8 . In the case of cyclodextrins, α -CD does not form an inclusion complex, whereas β -CD forms a 1:1 inclusion complex with the protonated form of the drug, and the binding affinity of EPT with β -CD is less compared to CB_7/CB_8 . Interestingly, in the case of γ -CD, drug exists in different forms depending on the concentration of the host. At lower concentration of γ -CD, 1:1 inclusion complex formation takes place and EPT exists in protonated form due to accessibility of water by the drug in the inclusion complex, whereas, at higher concentration, a 2:1 inclusion complex (γ -CD:EPT) is observed, in which EPT is completely buried inside the hydrophobic cavity of the capsule formed by two γ -CD molecules, and we believe the hydrophobic environment inside the capsule stabilizes the neutral form of the drug in the 2:1 inclusion complex. Deep insight into the molecular picture of these host–guest interactions has been provided by the docking studies followed by quantum chemical calculations.



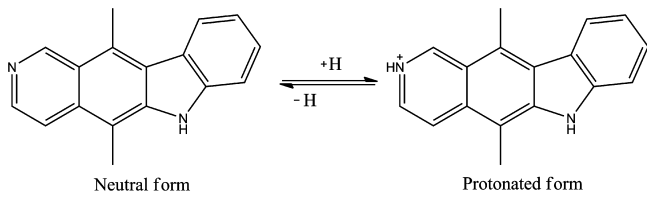
INTRODUCTION

Ellipticine (*S,N*-dimethyl-6*H*-pyrido[4,3-*b*]carbazole), a pyridocarbazole alkaloid that was first isolated from the leaves of *Ochrosia elliptica* by Goodwin et al. in 1959,¹ is an important drug owing to its antitumor and anti-HIV activities.^{2–4} Ellipticine (EPT) and its derivatives effectively intercalate in DNA and inhibit the activity of DNA topoisomerase-II, which ultimately restricts the process of DNA replication, and thus the transcription process of RNA.^{5–7} Ellipticine is known to interact with both DNA and topoisomerase-II through the formation of a DNA–ellipticine–topoisomerase-II ternary complex. EPT (Scheme 1) contains a basic, pyridine-like nitrogen with a protonation $\text{p}K_a$ of 7.4;^{8,9} hence, it exists in different prototropic forms depending on the pH as well as environmental polarity. Studies in living cells have revealed that ellipticine exists as a neutral form in cell cytoplasm, whereas in

the nucleus only the protonated form subsists.⁹ Although ellipticine is considered as one of the potential antitumor drugs, the major disadvantages in the usage of ellipticine in pharmaceuticals are its toxicity and low solubility in aqueous solution. The problems have been circumvented by attaching the drug to polymer, micelle, vesicle, liposome, and reverse micelle.^{10–15} Researchers also tried to enhance the solubility of the drug by encapsulating it inside cyclodextrin,^{8,16} which is considered as a potential drug carrier.¹⁷

To get insight into how ellipticine is transported to a tumor cell, it is necessary to establish a relationship between the environment and the photophysical properties of ellipticine. In continuation of this effort, researchers have investigated photophysical properties in bulk solvents, micelles, liposomes, and reverse micelles.^{10–15} EPT in non-polar and aprotic polar solvents exists in neutral form, and exhibits an emission peak in the range 410–440 nm.¹² Ellipticine exists as a protonated form (the $\text{p}K_a$ value of pyridine nitrogen is 7.4^{8,9}) in aqueous medium and emits at ~530 nm, whereas in methanol and ethylene glycol the drug exhibits concomitant dual emission at ~430 and ~510 nm.^{12,18,19} Miskolczy et al. assigned the red edge emission of EPT to excited state protonation of the

Scheme 1. Different Prototropic Forms of Ellipticine



Received: August 19, 2013

Revised: September 28, 2013

Published: October 18, 2013

pyridine moiety by solvent, instead of intramolecular proton transfer from the pyrrole ring to the pyridine ring.¹⁹ Fung et al. highlighted high polarity and dipole moments (higher than 12.2 D) along with a strong hydrogen bonding ability as the origin of higher wavelength peak.¹² Very recently, Banerjee et al. reported solvent mediated excited state intramolecular proton transfer from the pyrrole nitrogen to pyridine nitrogen as the origin of fluorescence form protonated EPT.¹⁸ Fluorescence measurements indicate that protonation and deprotonation of EPT are hampered in micelles.¹³ The entrapment of EPT in DPPC liposomes and its release has been monitored by steady state and time-resolved spectroscopic techniques, and it was found that release of the drug from liposome depends on the degree of penetration of bile salts.¹⁴ The photophysical studies of EPT in water and methanol reverse micelles indicate that ellipticine molecules are entrapped as a cationic form in water reverse micelles, whereas in the case of methanol reverse micelles cationic EPT is converted to neutral form.¹⁵

As macrocyclic host molecules act as drug carriers, drug solubilizers, and drug stabilizers,^{17,20–22} a few studies of EPT are also attempted in the macrocyclic hosts. The inclusion complexation between EPT and cyclodextrins has been monitored by steady state fluorescence, T-jump method. It was observed that β -CD forms a 1:1 inclusion complex with EPT, whereas γ -CD forms a 2:1 inclusion complex in a two-step process.^{8,16} Although the kinetics and thermodynamics are well explored in the above-mentioned studies, the photophysics are not well examined. Moreover, the dynamic aspect, which provides deep insight about the complex formation process, has not been addressed in their study. Among the macrocyclic hosts, recently cucurbituril emerges as a promising molecular container due to its versatile receptor properties.^{23,24} Cucurbiturils (CBn) contain glycoluril monomer units joined by pairs of methylene bridges and have barrel shaped structures with two identical carbonyl-laced portals.^{23,24} These macrocyclic hosts provide different cage diameters ranging from 4.5 to 12.5 Å for $CB5$ to $CB10$, respectively, and hence, guest molecules of various sizes can be encased by the CBn nanocavity.^{24,25} The internal hydrophobic cavity is responsible for the complexation with guest molecules by hydrophobic interactions, whereas the two portals of CBn lined by ureido carbonyl groups give an extra stability through ion–dipole and (or) hydrogen bonding interactions.^{23–29} Recent reports about the nontoxic behavior of CBn provide a boost for the use of CBn as a potential drug carrier.^{30–32} Herein, we have extensively studied the interaction behavior between EPT and cucurbiturils with the help of steady state, time-resolved fluorescence techniques, and compared the results with those of cyclodextrins. Finally, the docking and semiempirical quantum chemical calculations have been employed in deciphering the molecular pictures of the interactions between EPT and macrocyclic hosts (CBn , CDs).

■ EXPERIMENTAL SECTION

Ellipticine (EPT), cucurbit[n]uril (CBn), and cyclodextrins (CDs) were purchased from Sigma-Aldrich and used without further purification. Millipore water was used for sample preparation. The concentration of EPT in water was adjusted to $\sim 10^{-5}$ M using the reported value of the molar extinction coefficient ($\epsilon_{300} = 39\,000\text{ M}^{-1}\text{ cm}^{-1}$).³³ CBn /CD was gradually added to the solution containing EPT, and the solution was gently shaken after each addition of CBn /CD until completely

solubilized. Moreover, we have given 20 min of equilibration time after each addition of CBn /CD.

Absorbance measurements were performed in a Perkin-Elmer UV-visible spectrophotometer (Lambda-4S), and steady-state fluorescence spectra were recorded in a FluoroMax-4 spectrofluorimeter (Horiba Scientific, USA). All time-resolved fluorescence measurements were collected on a time correlated single photon counting (TCSPC) spectrometer (Horiba Jobin Yvon IBH, U.K.). The detailed description of the instrument is described elsewhere.^{34–36} Here, we have used a 375 nm diode laser for exciting drug molecules. Lifetime analysis was done by IBH DAS6 analysis software. We have fitted both lifetime data with a minimum number of exponential. The quality of each fitting was judged by χ^2 values and the visual inspection of the residuals. The value of $\chi^2 \approx 1$ was considered as the best fit for the plots.

■ RESULTS AND DISCUSSION

Steady-State Measurements. Absorption spectra of EPT in the absence and presence of CBn are shown in Figure 1. Drug in water (pH 6.5) exhibits absorbance in the 250–450 nm region with the absorbance maximum at 300 nm, which is believed to be the characteristic peak of the protonated form of EPT.^{8,9} Upon addition of $CB6$, absorption profiles do not change significantly, except the absorbance at 300 nm slightly decreases. However, with gradual addition of $CB7/CB8$, the absorption peak shows a bathochromic shift from 300 to 308 nm along with decrement in absorbance. These noteworthy changes in absorption features suggest strong binding interactions between EPT and CBn in the ground state.

To get clear insight about the complexation process, we have monitored emission profiles of EPT in the presence of cucurbiturils having various cavity sizes (Figure 2). EPT in aqueous solution exhibits a broad and unstructured peak at 530 nm, which is the signature peak of protonated EPT.¹⁰ Upon addition of $CB6$, the fluorescence intensity of EPT at 530 nm slightly increases, whereas a huge intensity increment is observed along with hypsochromic shift (Figure 2) upon addition of both $CB7$ and $CB8$. As the extent of peak enhancement in the presence of both $CB7$ and $CB8$ is more than that of $CB6$, it indicates that the interaction between drug and host is stronger in the case of both $CB7$ and $CB8$. The blue shift in emission spectra further confirms the formation of an inclusion complex between protonated EPT and CBn ($CB7/CB8$). It is also noticeable that the extent of blue shift in the case of $CB8$ is lesser compared to $CB7$, which can be attributed to the lower extent of hydrophobic interaction inside the $CB8$ cavity due to its larger cavity size than that of $CB7$. Here it is pertinent to mention that the average distance between 5-methyl and 11-methyl groups in EPT is 7 Å, while the inner diameters of the cavity of $CB6$, $CB7$, and $CB8$ are 5.8, 7.3, and 8.8 Å, respectively. The $CB6$ cavity is too small to accommodate EPT from the pyridine ring side. However, it can encapsulate EPT from the indole side, which would result in a blue shift in fluorescence spectra, as it is known that polarity change affects indole emission.³⁷ As a result, EPT cannot form an inclusion complex with $CB6$.

Considering the inner cavity sizes of both $CB7$ and $CB8$, it is possible that EPT can be encapsulated from the pyridine ring side. The increased intensity suggests that the non-radiative decay pathway, which arises due to free rotations of two methyl groups of drug, is reduced upon complexation with $CB7/CB8$. The intensity hike may also be attributed to the pK_a shift of

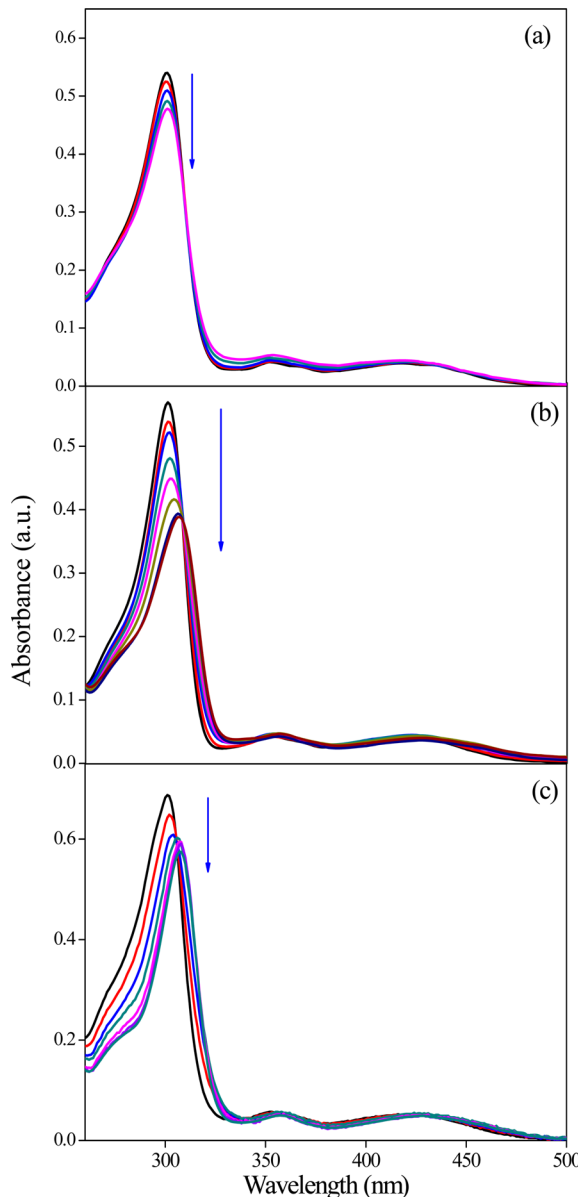


Figure 1. Absorption spectra of EPT ($15 \mu\text{M}$) in the presence of (a) CB6 (from 0 to $50 \mu\text{M}$), (b) CB7 (from 0 to $700 \mu\text{M}$), and (c) CB8 (from 0 to $100 \mu\text{M}$).

pyridine nitrogen as an outcome of inclusion complexation, because there are reports about the $\text{p}K_a$ shift of the drugs during inclusion complexation with cucurbituril.^{38–40} In EPT-CB7/-CB8 complex, the pyridine nitrogen resides at the portal, and therefore, its $\text{p}K_a$ value increases above 7.4. In order to verify whether the excited state $\text{p}K_a$ of ellipticine in the presence of CB n is affected or not, we have determined the excited state $\text{p}K_a$ with the help of the Förster cycle.⁴¹ We have verified that the excited state $\text{p}K_a$ increases to 9.5 in the presence of $500 \mu\text{M}$ CB7. Therefore, we believe the $\text{p}K_a$ shift of EPT also contributes toward the stability of drug in the inclusion complexes with CB n . It is also noticeable that a new peak at 440 nm appeared in addition to the 530 nm peak, particularly at a higher concentration of CB7. Note that neutral EPT exhibits an emission peak in the range 410–440 nm in non-polar solvents.¹² The appearance of the 440 nm peak at higher CB7 concentration infers that few drug molecules are

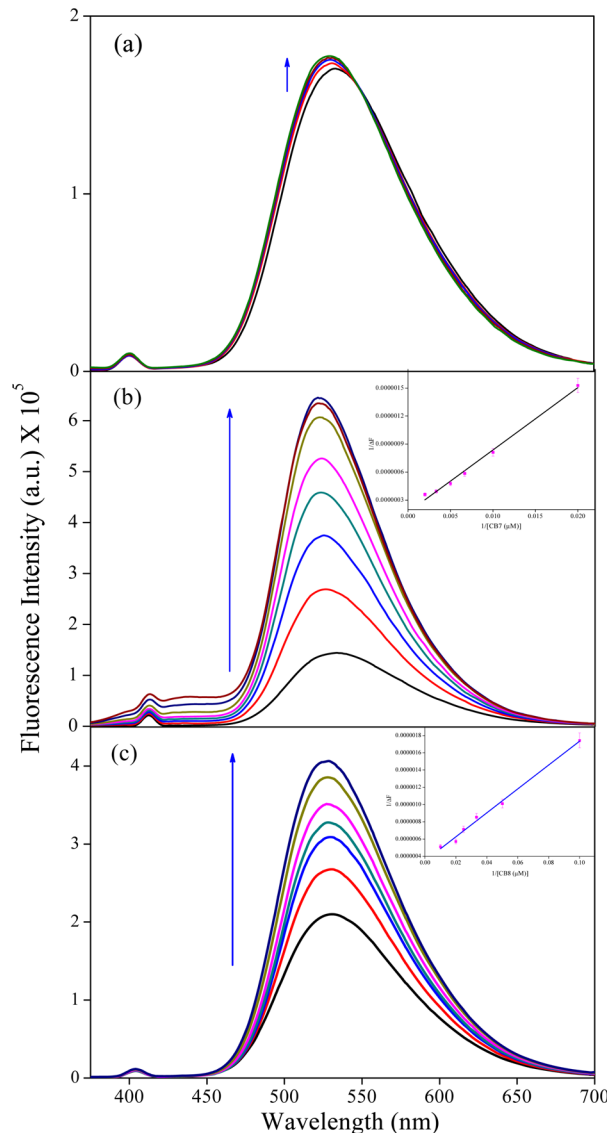


Figure 2. Emission spectra of EPT ($15 \mu\text{M}$) in the presence of (a) CB6 (from 0 to $50 \mu\text{M}$), (b) CB7 (from 0 to $700 \mu\text{M}$), and (c) CB8 (from 0 to $100 \mu\text{M}$). The inset shows the Benesi–Hildebrand plot.

getting encapsulated in such a way that pyridine nitrogen stays inside the hydrophobic cavity instead of staying at the portal.

The stoichiometry as well as binding constants of the inclusion complexes are determined from the fluorescence intensity using the Benesi–Hildebrand (BH) equation⁴²

$$\frac{1}{F - F_0} = \frac{1}{K(F_1 - F_0)[\text{host}]} + \frac{1}{F_1 - F_0} \quad (1)$$

where F_0 , F , and F_1 are the fluorescence intensities of EPT in the absence of host, in the presence of host, and in the inclusion complex, respectively. The double reciprocal plot monitored at 530 nm is observed to be linear ($R = 0.997$) for both CB7 (Figure 2b, inset) and CB8 (Figure 2c, inset), indicating formation of a 1:1 inclusion complex between EPT and CB n , and the association constants (K_1) are estimated to be 2.9×10^4 and $2.1 \times 10^5 \text{ M}^{-1}$, respectively.

Time-Resolved Measurements. Modulation in radiative properties of EPT upon interaction with CB n is clarified by fluorescence lifetime measurements. Fluorescence decays of EPT in the absence and presence of CB n collected at

corresponding emission maxima are shown in Figure 3, and fitting parameters are tabulated in Table S1 (Supporting

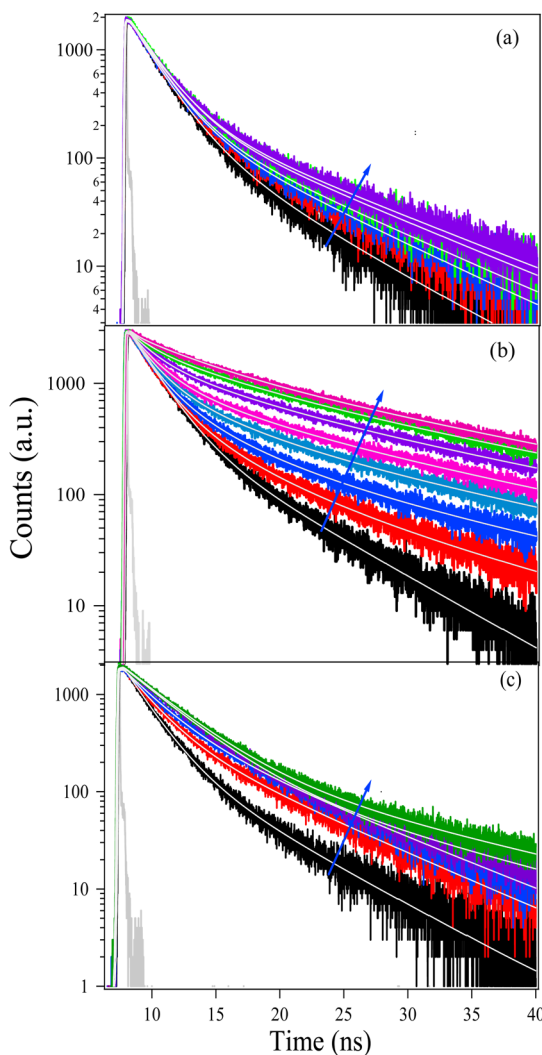


Figure 3. Fluorescence decay overlays of EPT ($15 \mu\text{M}$) in the presence of (a) CB6 (from 0 to $50 \mu\text{M}$), (b) CB7 (from 0 to $700 \mu\text{M}$), and (c) CB8 (from 0 to $100 \mu\text{M}$) collected at 530 nm ($\lambda_{\text{ex}} = 375 \text{ nm}$).

Information). At 530 nm , the drug exhibits biexponential decay in water having lifetime components of $\sim 2 \text{ ns}$ (84%) and $\sim 6.5 \text{ ns}$ (16%) with an average lifetime of $\sim 2.7 \text{ ns}$. It is hard to assign each of the above-mentioned lifetime components; hence, we will consider the average lifetime instead of focusing on individual components. The average lifetime of EPT in the presence of CB6 increases from 2.7 to 3.21 ns . As we have already explained that CB6 cannot accommodate the drug, the slight change in lifetime may be due to the ion–dipole/hydrogen bond interaction between EPT molecule (protonated) and carbonyl portals of CB6. This will be further verified by time-resolved anisotropy measurement. In the presence of CB7, the average lifetime increases from 2.7 to 10.3 ns at maximum CB7 concentration ($700 \mu\text{M}$), whereas the fluorescence lifetime of protonated EPT increases to 4.85 ns in the presence of $100 \mu\text{M}$ CB8 (Table S1, Supporting Information). These noteworthy changes in lifetime further confirm the inclusion complex formation between EPT and CB7/CB8. The increase in lifetime of EPT on complexation with CB n (Table S1, Supporting Information) can be

rationalized in terms of alterations in the radiative and non-radiative decay pathways (eq 2) of the drug due to their interaction with the macrocyclic host.

$$\frac{1}{\tau_f} = k_r + k_{\text{nr}} \quad (2)$$

Increased average lifetime (Table S1, Supporting Information) and enhancement in intensity of EPT in the presence of CB7/CB8 (Figure 3) suggest the decrease in non-radiative decay rate of EPT inside the nanocavity of CB7/CB8. We believe that the rotational motions of two methyl groups of EPT are restricted inside the nanocavity of CB n ; subsequently, the fast non-radiative relaxation channel of the drug is arrested. A longer fluorescence lifetime component of $10\text{--}20 \text{ ns}$ appeared in the presence of CB n hosts, indicating stability gained by the EPT upon encapsulation. The increased stability of protonated EPT inside the CB n nanocavity may be attributed mainly to the ion–dipole interactions between protonated EPT and carbonyl portals of CB n .

Time resolved anisotropy data provides information about the effect of microenvironment on rotational motions of the fluorophore, and hence, it can be used to probe the encapsulation process of EPT with cucurbituril. Anisotropy decay profiles of EPT in water and in the presence of various host molecules are shown in Figure 4. At 530 nm , EPT exhibits single exponential anisotropy decay in water with a rotational relaxation time of 120 ps . In the presence of host, the rotational relaxation time (τ_r) of EPT increases owing to increased rigidity due to formation of an inclusion complex with the host. In the presence of CB6, the τ_r value is estimated to be 130 ps , which is almost equal to that of EPT in water (120 ps). Hence, anisotropy results support our conjecture that EPT does not form an inclusion complex with CB6. In the presence of CB7 and CB8, the τ_r values of EPT are found to be 565 and 355 ps , respectively, inferring that EPT gets encapsulated by the above-mentioned macrocyclic hosts. The anisotropy results also suggest that EPT feels a more restricted environment inside the CB7 cavity compared to CB8, due to the smaller cavity size of the former host. Thus, anisotropy results support our steady state observations, where we have observed more vivid changes for CB7 compared to CB8. The orientation of EPT in the inclusion complexes can be better understood from docking followed by quantum chemical calculations, which are discussed in the later part of the manuscript.

Comparison of Binding Affinity and Photophysics of EPT between Cyclodextrin (CD) and CB n . The significance of the CB n –EPT binding interaction is better understood when the above results are compared with those of cyclodextrins (Figure 5; Figures S1–S4 and Table S2, Supporting Information) having similar cavity sizes. The steady state results obtained for CD are briefly explained here, as they are already reported.^{8,16} However, the dynamic aspect, which provides deep perception to these binding processes, has not been addressed previously. Here, we mainly focus on the dynamics of EPT in the presence of α -, β -, and γ -CD with the help of time-resolved fluorescence measurements (Figure 5c; Figures S3 and S4 and Table S2, Supporting Information). It has already been reported that EPT does not form an inclusion complex with α -CD,¹⁶ and we have also observed that the average lifetime of protonated EPT slightly changes from 2.7 ns in water to 3.24 ns in the presence of 20 mM α -CD. Thus, lifetime results also support that EPT does not form an inclusion complex with α -CD. Our studies showed that EPT

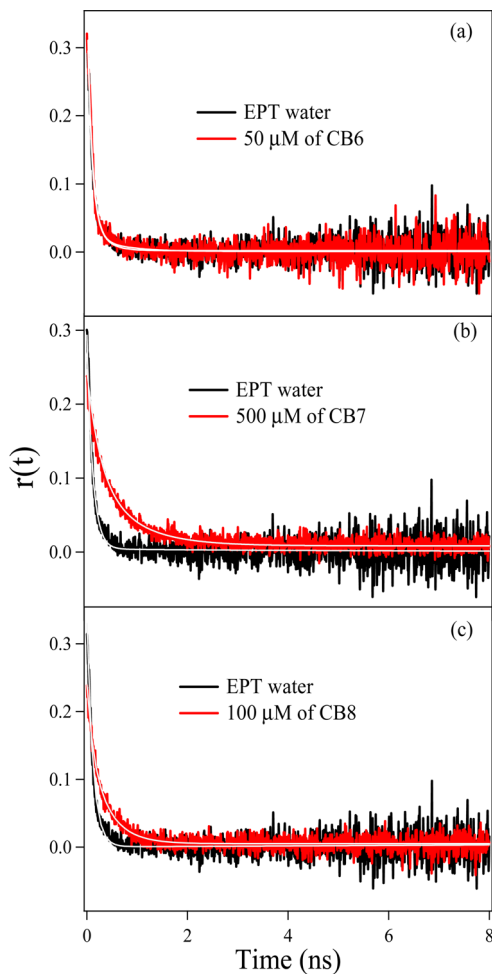


Figure 4. Anisotropy decay overlays of EPT (15 μM) at 530 nm in the presence of (a) CB6 (from 0 to 50 μM), (b) CB7 (from 0 to 0.5 mM), and (c) CB8 (from 0 to 100 μM) collected at the emission maximum ($\lambda_{\text{ex}} = 375 \text{ nm}$).

also does not form any inclusion complex with CB6, which has a comparable cavity size of α -CD. In the presence of β -CD, the average lifetime of protonated EPT increases up to 3.6 ns, and is consistent with the intensity hike in emission spectra. The lifetime data in the presence of β -CD is devoid of the ~ 10 ns component, which appears in the presence of CB7 having a similar cavity size. Moreover, the changes in lifetime as well as intensity are significantly higher in the case of CB7, though the concentration of CB7 is a few-fold lower than that of β -CD. Hence, we believe the hydrophobic cavities of both CB7 and β -CD are not responsible for the modulation of photophysics of EPT; rather, the different topology of the upper and lower rims of both of the hosts is accountable for the modulation of photophysics of EPT to different extents. Cyclodextrins having a hydrophobic cavity and hydroxyl groups in the rims encapsulate guest molecules mainly through hydrophobic as well as hydrogen bond interactions.^{43,44} On the other hand, owing to carbonyl-lined portals, the binding interaction with CB7 takes place mainly through ion–dipole interaction, and it is quite likely that the protonated form of EPT interacts with the electron rich carbonyl portal through the positive charge developed on the pyridine moiety. Therefore, EPT gains extra stability in the inclusion complex with CB7. As an outcome of the above-mentioned effects, EPT exhibits more vivid changes

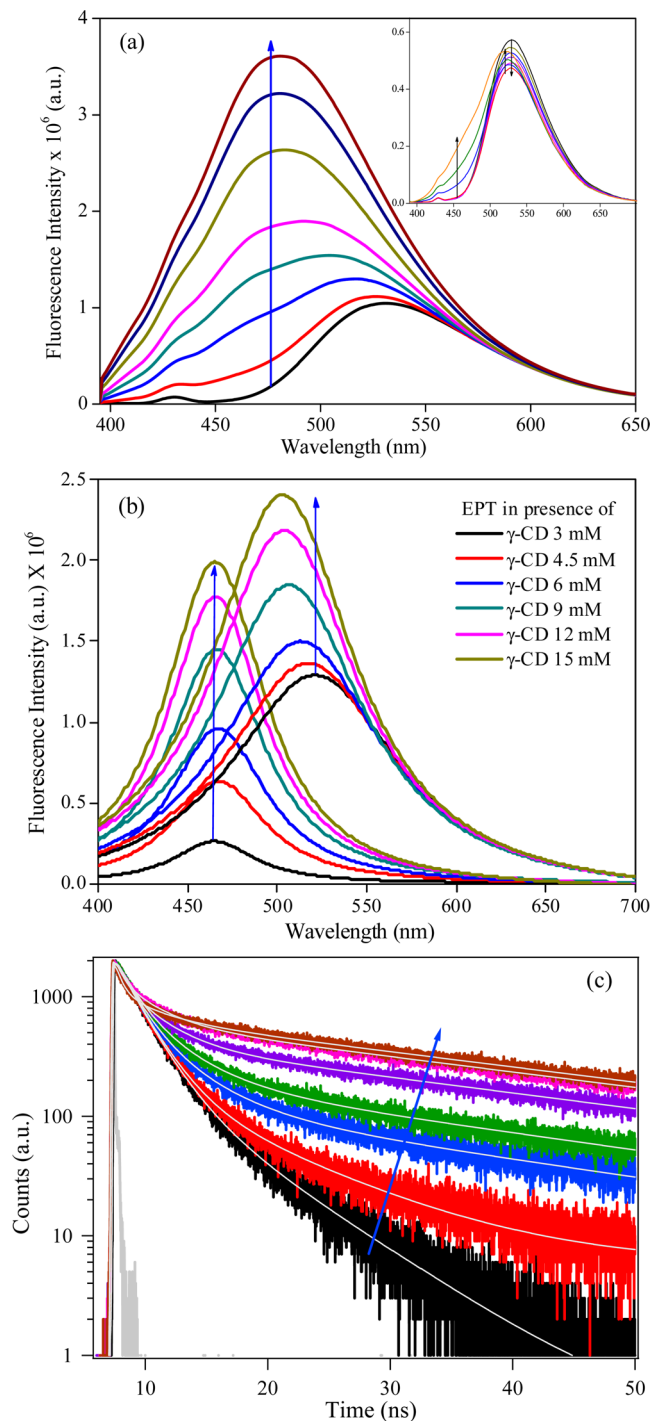


Figure 5. Emission spectra of EPT (15 μM) in the presence of γ -CD (0–15 mM): (a) original; (b) Lorenzian multipeak fits. (c) Fluorescence transients of EPT in the presence of γ -CD (0–15 mM) collected at 530 nm ($\lambda_{\text{ex}} = 375 \text{ nm}$). The inset in part a shows emission spectra of EPT at a lower concentration of γ -CD (0–1 mM).

in steady state as well lifetime profiles in the presence of CB7 compared to β -CD.

Interestingly, the emission profiles of the drug in the presence of γ -CD are significantly different from other macrocyclic hosts. In the presence of γ -CD, a marked increase in the emission intensity of EPT accompanied by a hypsochromic shift of ~ 50 nm is observed. Moreover, a peaking hump is generated at 475 nm around 300 μM γ -CD

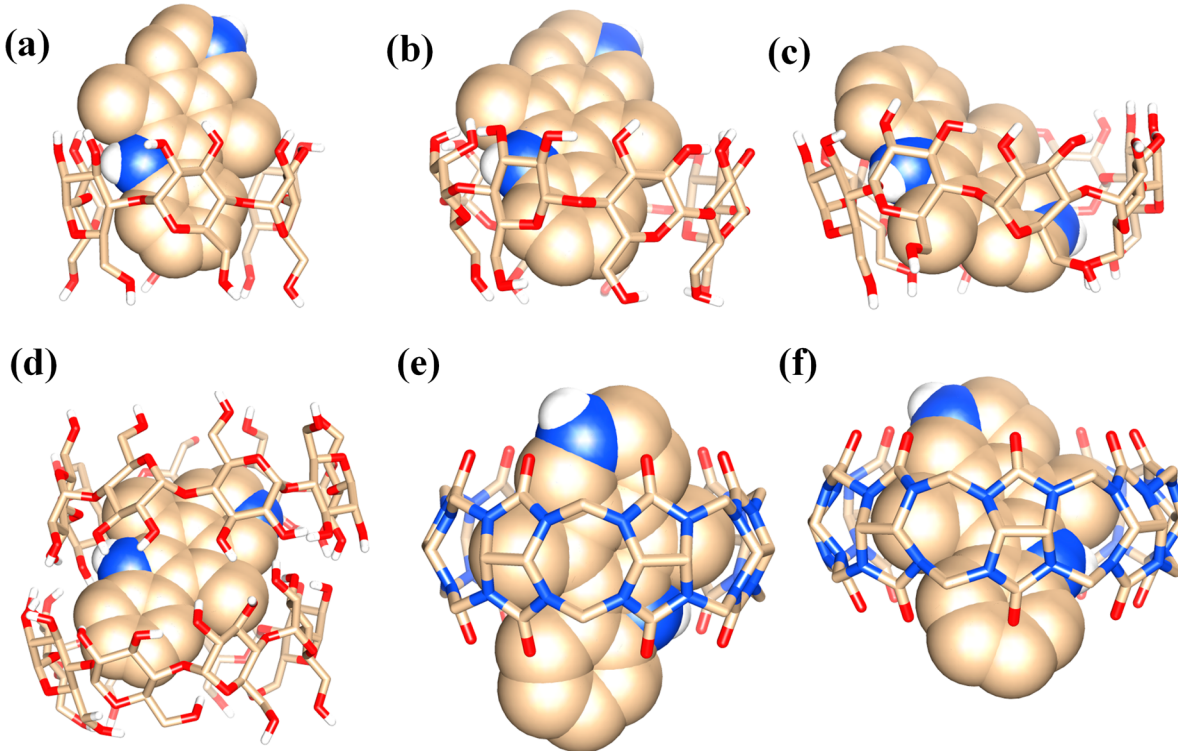


Figure 6. Optimized structure of (a) docked α -CD:EPT complex (1:1), (b) docked β -CD:EPT complex (1:1), (c) docked γ -CD:EPT complex (1:1), (d) docked γ -CD:EPT complex (2:1), (e) docked CB7:EPT complex (1:1), and (f) docked CB8:EPT complex (1:1).

(Figure 5a, inset) and the emission spectra become broad at higher concentration, exhibiting an emission maximum at 480 nm (Figure 5a). Although a similar observation has been reported by other groups, the detailed interpretation of the spectra has not been addressed previously. In order to get clear perception about the spectral features, we have deconvoluted the emission spectra using Lorenzian fitting in the presence of γ -CD (Figure 5b). It is clearly seen from the deconvoluted spectra that a new peak appeared at \sim 480 nm along with the main peak at \sim 530 nm at a higher concentration of γ -CD. The peak position at 480 nm remains the same, although a huge increment in intensity is observed as the γ -CD concentration increases, whereas the peak at 530 nm is gradually blue-shifted along with the slight increase in intensity. The 530 nm peak definitely indicates the presence of a protonated form of EPT, and the blue shift confirms the encapsulation of protonated EPT inside the γ -CD nanocavity. The 480 nm peak may be ascribed to the neutral form of EPT inside the γ -CD nanocavity, as the neutral form generally exhibits an emission maximum well before 450 nm.¹² The high bathochromic shift in the presence of γ -CD may appear from the caging effect by the host. The binding interaction between the EPT and γ -CD is further examined by monitoring the fluorescence intensity of the drug with increasing concentration of the macrocyclic host. It is clearly noticeable that the titration curve (monitored at 530 nm) significantly deviates from linearity (Figure S2c, Supporting Information), pointing toward the formation of multiple inclusion complexes between host and guest. Moreover, a slope change is observed in the titration curve at around 300 μ M. In fact, there is a report about the stepwise multiple inclusion complexation between EPT and γ -CD. On the basis of our titration curve as well as from a literature report, it is reasonable to assume that 1:1 complexation equilibrium exists

until 300 μ M γ -CD concentration, and thereafter, 2:1 (γ -CD:EPT) inclusion complexation dominates. The stoichiometries are further confirmed by BH plot (Figure S3, Supporting Information). It is already reported that the interaction between EPT and γ -CD occurs in two steps, the first one involving the encapsulation pyridine residue of the drug and the second being the inclusion of 1:1 inclusion complex by another cyclodextrin from the indole side.⁸ Therefore, on the basis of our observation as well as literature reports, we envisage that the pyridine ring resides at the rim in the 1:1 inclusion complex, where it can access water. As a result, EPT prevails as the protonated form in the 1:1 inclusion complex. On the other hand, pyridine nitrogen of EPT is prevented from exposure to water in the 2:1 inclusion complex, as the second cyclodextrin molecule acts as a cap for the 1:1 inclusion complex.

The modulation in the radiative properties of EPT on interaction with γ -CD is also clarified by the fluorescence lifetime measurements (Figure 5c). We have collected the fluorescence lifetime of EPT in the presence of γ -CD at the corresponding emission maximum. In the presence of γ -CD, the fluorescence lifetime of EPT increases hugely from 2.7 to 10.36 ns (Table S2, Supporting Information). This 4-fold enhancement in fluorescence lifetime of EPT supports a high binding affinity of γ -CD with EPT compared to other macrocyclic hosts (α -CD, β -CD). Moreover, with the addition of γ -CD, a new component with longer lifetime (25–35 ns) arises at \geq 300 μ M and its contribution increases with gradual addition of γ -CD. A similar lifetime component for EPT was observed in non-polar solvents where the neutral form predominantly exists in the solution. Therefore, we believe that the long component that appeared in the decay profile is attributed to the neutral form of EPT, and is corroborative with steady state results where we have observed the formation of

the neutral form of EPT in the presence of γ -CD when the 2:1 (γ -CD:EPT) inclusion complex is formed.

To further scrutinize the complexation processes with CDs, we have collected anisotropy decay profiles for EPT at the emission maximum in the presence of CDs (Figure S5, Supporting Information). As we have already stated, EPT exhibits single exponential anisotropy decay in water with a rotational correlation time of 120 ps. In the presence of α -CD, the τ_r value is estimated to be 170 ps, which is not significantly higher than that of EPT in water (120 ps). Hence, anisotropy results support that EPT does not form an inclusion complex with α -CD. However, in the presence of β -CD and γ -CD, the τ_r values of EPT are found to be 520 and 855 ps, respectively, affirming the formation of inclusion complexes between drug and the above-mentioned macrocyclic hosts. The longer rotational relaxation time scale in the presence of 15 mM γ -CD further supports the formation of a 2:1 inclusion complex (γ -CD:EPT), in which the drug molecule feels additional rigidity by a second host molecule, which acts as a cap toward the 1:1 inclusion complex.

To compare the binding affinity of the drug between CDs and CB_n , we have determined binding constants using BH plots (Figure S3, Supporting Information), and the values are estimated to be 104 M^{-1} , $2.8 \times 10^4 \text{ M}^{-1}$, and $1.5 \times 10^5 \text{ M}^{-2}$ for β -CD:EPT, γ -CD:EPT, and γ -CD:EPT: γ -CD inclusion complexes, respectively. On the other hand, the association constant between EPT and CB_n is varied from 2.9×10^4 to $2.1 \times 10^5 \text{ M}^{-1}$, indicating cucurbiturils have a higher binding affinity toward EPT compared to CDs. This higher binding affinity may be attributed to the strong ion–dipole interactions of protonated EPT with carbonyl portals of CB_n which are absent in CDs.

Docking and Quantum Chemical Calculations. To obtain a molecular picture of orientation of EPT in the inclusion complexes as well as to gain insight into the stabilization achieved due to encapsulation, we have docked the drug (EPT) into the host molecules (CDs and CB_n), followed by a semiempirical quantum chemical optimization. The docking has been performed using AutoDock (4.2) software,⁴⁵ and the detailed docking protocol was described elsewhere.^{36,40} Initially, all the chemical structures (hosts and guest) are geometry optimized using DFT-B3LYP with the 6-31G* basis set in Gaussian 09.⁴⁶ During docking, the receptor was kept rigid and the ligand was flexible. Following the experimental findings, we have taken the protonated form of EPT for all the docking studies, except in the case of γ -CD, in which the neutral form of the drug has also been considered during docking study. In the case of γ -CD, we have docked EPT (protonated form) and γ -CD to get a 1:1 (γ -CD:EPT) inclusion complex. In order to get a 2:1 (γ -CD:EPT) inclusion complex, we have docked a 1:1 (γ -CD:EPT) inclusion complex with neutral EPT to another γ -CD. Finally, all the inclusion complexes obtained from docking studies are further optimized using Gaussian 09 software⁴⁶ at the PM3MM level. Since the docking and geometry optimization were done without consideration of any solvent and other parameters, these geometries provide only a qualitative picture of the structures in the ground state. Optimized structures of the various inclusion complexes are shown in Figure 6. We have evaluated the interaction energy for all plausible complexes by subtracting the heat of formation of individual molecules from the complex.^{36,40} Although the docking study indicates the formation of an inclusion complex between EPT and α -CD (Figure 6a), the

interaction energy obtained from the quantum chemical optimization method is positive (5 kcal mol⁻¹), which indicates that energetically EPT does not prefer to be included inside the cavity of α -CD, probably due to the smaller size of the host cavity. Therefore, theoretical calculation supports our experimental findings that EPT does not form an inclusion complex with α -CD. In the case of β -CD, the interaction energy is negative (-29 kcal mol⁻¹), suggesting that 1:1 inclusion complex formation between EPT and β -CD is energetically feasible. For γ -CD, both the 1:1 and 2:1 (γ -CD:EPT) inclusion complexes are energetically feasible by -23 and -35 kcal mol⁻¹, respectively. It is important to note that these two types of inclusion complexes in the case of γ -CD were predicted previously by Chahine et al.,⁸ and our experimental observation also infers the formation of stepwise multiple inclusion complexation between EPT and γ -CD. It is clear from the geometry optimized structure of the 1:1 inclusion complex with γ -CD that entry of EPT takes place from the pyridine side in such a way that pyridine rings of EPT are still accessible to the water environment, which favors the existence of the cationic form of EPT (Figure 6c). However, in the case of the 2:1 (γ -CD:EPT) inclusion complex, the EPT is completely buried inside the capsule formed by two γ -CD molecules and the pyridine ring is totally protected from water (Figure 6d). Hence, protonation is not feasible in this case, and as a result, EPT exists as the neutral form in this 2:1 inclusion complex. The hydrophobic environment inside the capsule is believed to stabilize the neutral form of EPT. Theoretical studies fully support our conjecture drawn from experimental results that EPT exists as the protonated form in the 1:1 (γ -CD:EPT) inclusion complex formed in the lower concentration regime of the host, whereas it subsists as the neutral form in the 2:1 inclusion complex at the higher concentration regime of γ -CD.

If we compare the complexation of EPT with CDs and CB_n , the orientation of EPT inside the nanocavity of CDs is different from that in the CB_n cavity. Heat of formations for inclusion complexes of EPT with CB7 and CB8 are -42 and -48 kcal mol⁻¹, respectively. From these energy values, it is clear that the complex formation of EPT with CB_n is energetically more favorable than that with CDs. EPT orients inside CB_n (7 and 8) in such a way that the pyridine moiety resides at the carbonyl portals of CB_n , so that it is further stabilized through ion–dipole interaction (Figure 6e,f). This additional binding interaction of EPT with CB_n leads to the relatively higher interaction energies with CB_n compared to CDs. Moreover, in this orientation, there is a possibility for the increase in pK_a of pyridine nitrogen due to the surrounding electron rich carbonyl portals. Furthermore, in this orientation, the EPT can access the water environment, which causes protonation of EPT in the inclusion complexes formed by CB_n .

CONCLUSION

In this work, the interaction behavior between an anticancer drug EPT and cucurbiturils has been demonstrated with the help of absorption, steady state fluorescence, and time-resolved fluorescence techniques. For comparison, we have done similar experiments using conventional hosts, cyclodextrins. Our experimental results indicate the formation of 1:1 inclusion complexation of EPT with CB7 and CB8, and the protonated form of EPT gets stabilized mainly through the ion–dipole interaction between host and positively charged drug. On the other hand, drug does not form an inclusion complex with CB6. Among cyclodextrins, α -CD does not form an inclusion

complex with the drug, whereas β -CD forms a 1:1 inclusion complex with the protonated form of the drug. Notably, the binding affinity for β -CD is less compared to CB7/CB8. Interestingly, in the case of γ -CD, drug forms a stable 1:1 inclusion complex in its protonated form at a lower concentration of host, whereas drug is encapsulated by two γ -CD molecules at a higher concentration of host, and thereby drug exists in the neutral form at a higher concentration of γ -CD. Molecular docking as well as quantum chemical calculations were employed to get insight into the orientation of EPT drug inside the nanocavities of these macrocycles. The molecular pictures indicate that pyridine nitrogen of EPT is situated at the electron rich portal in the inclusion complexes with CB_n, and as a result, the basicity of quinoline nitrogen increases significantly. However, in the case of the 2:1 inclusion complex (γ -CD:EPT) with γ -CD, the EPT is completely buried inside the hydrophobic cavity of the capsule formed by two γ -CD molecules, and this hydrophobic environment stabilizes the neutral form of EPT which is not observed in other 1:1 inclusion complexes with CB_n and β -CD.

■ ASSOCIATED CONTENT

Supporting Information

Tables showing fluorescence decay transients and figures showing absorption and emission spectra, BH plots, fluorescence transients, and anisotropy decays. This material is available free of charge via the Internet at <http://pubs.acs.org>.

■ AUTHOR INFORMATION

Corresponding Author

*E-mail: p.hazra@iiserpune.ac.in. Phone: +91-20-2590-8077. Fax: +91-20-2589 9790.

Notes

The authors declare no competing financial interest.

■ ACKNOWLEDGMENTS

This work is partly supported by Council of Scientific and Industrial Research (CSIR), Government of India. A.S. is thankful to CSIR for a Senior Research Fellowship (SRF), and R.K.K. is thankful to University Grants Commission (UGC) for a Junior Research Fellowship (JRF). Authors thank Director, IISER-Pune, for providing excellent experimental and computation facilities. Authors are thankful to anonymous reviewers for their valuable comments and suggestions.

■ REFERENCES

- Goodwin, S.; Smith, A. F.; Horning, E. C. Alkaloids of Ochrosia Elliptica Labill. *J. Am. Chem. Soc.* **1959**, *81*, 1903–1908.
- Werbel, L. M.; Angelo, M.; Fry, D. W.; Worth, D. F. Basically Substituted Ellipticine Analogs as Potential Antitumor Agents. *J. Med. Chem.* **1986**, *29*, 1321–1322.
- Mathé, G.; Triana, K.; Pontiggia, P.; Blanquet, D.; Hallard, M.; Morette, C. Data of Pre-Clinical and Early Clinical Trials of Acriflavine and Hydroxy-Methyl-Ellipticine Reviewed, Enriched by the Experience of Their Use for 18 Months to 6 Years in Combinations with Other HIV1 Virostatics. *Biomed. Pharmacother.* **1998**, *52*, 391–396.
- Ding, L.; Balzarini, J.; Schols, D.; Meunier, B.; De Clercq, E. Anti-Human Immunodeficiency Virus Effects of Cationic Metalloporphyrin-Ellipticine Complexes. *Biochem. Pharmacol.* **1992**, *44*, 1675–1679.
- (5) Le Pecq, J.-B.; Nguyen-Dat-Xuong; Gosse, C.; Paoletti, C. A New Antitumoral Agent: 9-Hydroxyellipticine. Possibility of a Rational Design of Anticancerous Drugs in the Series of DNA Intercalating Drugs. *Proc. Natl. Acad. Sci. U.S.A.* **1974**, *71*, 5078–5082.
- (6) Ohashi, M.; Oki, T. Overview Oncologic, Endocrine & Metabolic: Oncologic, Endocrine & Metabolic:Ellipticine and Related Anticancer Agents. *Expert Opin. Ther. Pat.* **1996**, *6*, 1285–1294.
- (7) Arteaga, C. L.; Kisner, D. L.; Goodman, A.; Von Hoff, D. D. Elliptinium, a DNA Intercalating Agent with Broad Antitumor Activity in a Human Tumor Cloning System. *Eur. J. Cancer Clin. Oncol.* **1987**, *23*, 1621–1626.
- (8) El Hage Chahine, J. M.; Bertigny, J.-P.; Schwaller, M.-A. Kinetics and Thermodynamics of the Formation of Inclusion Complexes Between Cyclodextrins and DNA-Intercalating Agents. Inclusion of Ellipticine in [Gamma]-Cyclodextrin. *J. Chem. Soc., Perkin Trans. 2* **1989**, *0*, 629–633.
- (9) Sureau, F.; Moreau, F.; Millot, J. M.; Manfait, M.; Allard, B.; Aubard, J.; Schwaller, M. A. Microspectrofluorometry of the Protonation State of Ellipticine, an Antitumor Alkaloid, in Single Cells. *Biophys. J.* **1993**, *65*, 1767–1774.
- (10) Fung, S. Y.; Yang, H.; Bhola, P. T.; Sadatmousavi, P.; Muzar, E.; Liu, M.; Chen, P. Self-Assembling Peptide as a Potential Carrier for Hydrophobic Anticancer Drug Ellipticine: Complexation, Release and In Vitro Delivery. *Adv. Funct. Mater.* **2009**, *19*, 74–83.
- (11) Fung, S. Y.; Yang, H.; Chen, P. Formation of Colloidal Suspension of Hydrophobic Compounds with an Amphiphilic Self-Assembling Peptide. *Colloids Surf., B* **2007**, *55*, 200–211.
- (12) Fung, S. Y.; Duhamel, J.; Chen, P. Solvent Effect on the Photophysical Properties of the Anticancer Agent Ellipticine. *J. Phys. Chem. A* **2006**, *110*, 11446–11454.
- (13) Sbai, M.; Ait Lyazidi, S.; Lerner, D. A.; del Castillo, B.; Martin, M. A. Use of Micellar Media for the Fluorimetric Determination of Ellipticine in Aqueous Solutions. *J. Pharm. Biomed. Anal.* **1996**, *14*, 959–965.
- (14) Thakur, R.; Das, A.; Chakraborty, A. Photophysical and Photodynamical Study of Ellipticine: an Anticancer Drug Molecule in Bile Salt Modulated In Vitro Created Liposome. *Phys. Chem. Chem. Phys.* **2012**, *14*, 15369–15378.
- (15) Thakur, R.; Das, A.; Chakraborty, A. Fate of Anticancer Drug Ellipticine in Reverse Micelles in Aqueous and Methanolic Environment: A Photophysical Approach. *Chem. Phys. Lett.* **2013**, *563*, 37–42.
- (16) Sbai, M.; Lyazidi, S. A.; Lerner, D. A.; del Castillo, B.; Martin, M. A. Modified β -Cyclodextrins as Enhancers of Fluorescence Emission of Carbazole Alkaloid Derivatives. *Anal. Chim. Acta* **1995**, *303*, 47–55.
- (17) Uekama, K.; Hirayama, F.; Irie, T. Cyclodextrin Drug Carrier Systems. *Chem. Rev.* **1998**, *98*, 2045–2076.
- (18) Banerjee, S.; Pabbathi, A.; Sekhar, M. C.; Samanta, A. Dual Fluorescence of Ellipticine: Excited State Proton Transfer from Solvent versus Solvent Mediated Intramolecular Proton Transfer. *J. Phys. Chem. A* **2011**, *115*, 9217–9225.
- (19) Miskolczy, Z.; Biczók, L.; Jablonkai, I. Effect of Hydroxylic Compounds on the Photophysical Properties of Ellipticine and its 6-Methyl Derivative: The Origin of Dual Fluorescence. *Chem. Phys. Lett.* **2006**, *427*, 76–81.
- (20) Brewster, M. E.; Loftsson, T. Cyclodextrins as Pharmaceutical Solubilizers. *Adv. Drug Delivery Rev.* **2007**, *59*, 645–666.
- (21) Walker, S.; Oun, R.; McInnes, F. J.; Wheate, N. J. The Potential of Cucurbit[n]urils in Drug Delivery. *Isr. J. Chem.* **2011**, *51*, 616–624.
- (22) Gokel, G. W.; Leevy, W. M.; Weber, M. E. Crown Ethers: Sensors for Ions and Molecular Scaffolds for Materials and Biological Models. *Chem. Rev.* **2004**, *104*, 2723–2750.
- (23) Lee, J. W.; Samal, S.; Selvapalam, N.; Kim, H.-J.; Kim, K. Cucurbituril Homologues and Derivatives: New Opportunities in Supramolecular Chemistry. *Acc. Chem. Res.* **2003**, *36*, 621–630.
- (24) Lagona, J.; Mukhopadhyay, P.; Chakrabarti, S.; Isaacs, L. The Cucurbit[n]uril Family. *Angew. Chem., Int. Ed.* **2005**, *44*, 4844–4870.
- (25) Dsouza, R. N.; Pischel, U.; Nau, W. M. Fluorescent Dyes and Their Supramolecular Host/Guest Complexes with Macrocycles in Aqueous Solution. *Chem. Rev.* **2011**, *111*, 7941–7980.
- (26) Day, A. I.; Blanch, R. J.; Arnold, A. P.; Lorenzo, S.; Lewis, G. R.; Dance, I. A Cucurbituril-Based Gyroscane: A New Supramolecular Form. *Angew. Chem., Int. Ed.* **2002**, *41*, 275–277.

- (27) Czar, M. F.; Jockusch, R. A. Inside Cover: Understanding Photophysical Effects of Cucurbituril Encapsulation: A Model Study with Acridine Orange in the Gas Phase. *ChemPhysChem* **2013**, *14*, 1086–1086.
- (28) Wagner, B. D. Hydrogen Bonding of Excited States in Supramolecular Host-Guest Inclusion Complexes. *Phys. Chem. Chem. Phys.* **2012**, *14*, 8825–8835.
- (29) Tang, H.; Fuentealba, D.; Ko, Y. H.; Selvapalam, N.; Kim, K.; Bohne, C. Guest Binding Dynamics with Cucurbit[7]uril in the Presence of Cations. *J. Am. Chem. Soc.* **2011**, *133*, 20623–20633.
- (30) Hettiarachchi, G.; Nguyen, D.; Wu, J.; Lucas, D.; Ma, D.; Isaacs, L.; Briken, V. Toxicology and Drug Delivery by Cucurbit[n]uril Type Molecular Containers. *PLoS One* **2010**, *5*, e10514.
- (31) Uzunova, V. D.; Cullinan, C.; Brix, K.; Nau, W. M.; Day, A. I. Toxicity of Cucurbit[7]uril and Cucurbit[8]uril: an Exploratory In Vitro and In Vivo Study. *Org. Biomol. Chem.* **2010**, *8*, 2037–2042.
- (32) Ma, D.; Hettiarachchi, G.; Nguyen, D.; Zhang, B.; Wittenberg, J. B.; Zavalij, P. Y.; Briken, V.; Isaacs, L. Acyclic Cucurbit[n]uril Molecular Containers Enhance the Solubility and Bioactivity of Poorly Soluble Pharmaceuticals. *Nat. Chem.* **2012**, *4*, 503–510.
- (33) Zsila, F.; Kaman, J.; Boganyi, B.; Jozsvai, D. Binding of Alkaloids into the S1 Specificity Pocket of [Small Alpha]-Chymotrypsin: Evidence from Induced Circular Dichroism Spectra. *Org. Biomol. Chem.* **2011**, *9*, 4127–4137.
- (34) Sengupta, A.; Hazra, P. Solvation Dynamics of Coumarin 153 in SDS Dispersed Single Walled Carbon Nanotubes (SWNTs). *Chem. Phys. Lett.* **2010**, *501*, 33–38.
- (35) Sengupta, A.; Khade, R. V.; Hazra, P. How Does the Urea Dynamics Differ from Water Dynamics inside the Reverse Micelle? *J. Phys. Chem. A* **2011**, *115*, 10398–10407.
- (36) Gavvala, K.; Sasikala, W. D.; Sengupta, A.; Dalvi, S. A.; Mukherjee, A.; Hazra, P. Modulation of Excimer Formation of 9-(Dicyano-Vinyl)julolidine by the Macro cyclic Hosts. *Phys. Chem. Chem. Phys.* **2013**, *15*, 330–340.
- (37) Duuren, B. L. v. Solvent Effects in the Fluorescence of Indole and Substituted Indoles. *J. Org. Chem.* **1961**, *26*, 2954–2960.
- (38) Barooah, N.; Mohanty, J.; Pal, H.; Bhasikuttan, A. C. Supramolecular Assembly of Hoechst-33258 with Cucurbit[7]uril Macrocycle. *Phys. Chem. Chem. Phys.* **2011**, *13*, 13117–13126.
- (39) Ghosh, I.; Nau, W. M. The Strategic Use of Supramolecular pKa Shifts to Enhance the Bioavailability of Drugs. *Adv. Drug Delivery Rev.* **2012**, *64*, 764–783.
- (40) Gavvala, K.; Sengupta, A.; Hazra, P. Modulation of Photophysics and pKa Shift of the Anti-cancer Drug Camptothecin in the Nanocavities of Supramolecular Hosts. *ChemPhysChem* **2013**, *14*, 532–542.
- (41) Lakowicz, J. R. *Principles of Fluorescence Spectroscopy*, 3rd ed.; Springer Science: New York, 2006.
- (42) Benesi, H. A.; Hildebrand, J. H. A Spectrophotometric Investigation of the Interaction of Iodine with Aromatic Hydrocarbons. *J. Am. Chem. Soc.* **1949**, *71*, 2703–2707.
- (43) Rekharsky, M. V.; Goldberg, R. N.; Schwarz, F. P.; Tewari, Y. B.; Ross, P. D.; Yamashoji, Y.; Inoue, Y. Thermodynamic and Nuclear Magnetic Resonance Study of the Interactions of .Alpha.- and .Beta.-Cyclodextrin with Model Substances: Phenethylamine, Ephedrines, and Related Substances. *J. Am. Chem. Soc.* **1995**, *117*, 8830–8840.
- (44) Rekharsky, M. V.; Mayhew, M. P.; Goldberg, R. N.; Ross, P. D.; Yamashoji, Y.; Inoue, Y. Thermodynamic and Nuclear Magnetic Resonance Study of the Reactions of α - and β -Cyclodextrin with Acids, Aliphatic Amines, and Cyclic Alcohols. *J. Phys. Chem. B* **1997**, *101*, 87–100.
- (45) Morris, G. M.; Huey, R.; Lindstrom, W.; Sanner, M. F.; Belew, R. K.; Goodsell, D. S.; Olson, A. J. AutoDock4 and AutoDockTools4: Automated Docking with Selective Receptor Flexibility. *J. Comput. Chem.* **2009**, *30*, 2785–2791.
- (46) Frisch, M. J.; Trucks, G. W.; Schlegel, H. B.; Scuseria, G. E.; Robb, M. A.; Cheeseman, J. R.; Scalmani, G.; Barone, V.; Mennucci, B.; Petersson, G. A.; et al. *Gaussian 09*, rev. A.02; Gaussian, Inc.: Wallingford, CT, 2009.